Alexandria Engineering Journal 79 (2023) 556–567

Contents lists available at ScienceDirect

Alexandria Engineering Journal

journal homepage: www.elsevier.com/locate/aej

Original Article

Optimized shape for improved cooling of ventilated discs

Chengfeng Li [a], Hyun-Ik Yang [b,*]

[a] Department of Mechanical Design Engineering, BK21 FOUR ERICA-ACE Center, Hanyang University, 55, Hanyangdaehak-ro, Sangrok-gu, Ansan, Gyeonggi-do 15588, Republic of Korea

[b] Department of Mechanical Engineering, BK21 FOUR ERICA-ACE Center, Hanyang University, 55, Hanyangdaehak-ro, Sangrok-gu, Ansan, Gyeonggi-do 15588, Republic of Korea

ARTICLE INFO

Keywords:
Shape optimization
Ventilation plate
Cooling effect

ABSTRACT

During the braking process of a car, the temperature of the brake system increases continuously, and if the cooling performance of the brake system is insufficient, accidents can occur. For this reason, in this study, the experimental method of the Taguchi design was used to optimize the design of a ventilated brake disc with radial vanes using three design parameters (i.e., number of vanes, vane thickness, and steering angle), and the airflow and temperature distribution around the brake disc and tire were simulated using finite elements. The simulation results show that the solution in this study can increase the ventilation gap from 10 to 14 mm, the bending angle of the blades from 29° to 37°, and the cooling effect after emergency braking by 6.1% and 8.8%, respectively, when dissipating heat for 100 s at a driving speed of 60 km/h.

1. Introduction

The disc brake is a component attached to the wheel hub that rotates with it, forming the moving component of the braking system (see Fig. 1). On the surface or friction area of the disc brake, the brake discs interact with each other, such that the vehicle stops owing to the constant friction established between the brake disc and the brake pad. In this process, the hydraulic pump is enabled when the brake pedal starts, and the brake pedal delivers the brake fluid to the calipers. The pressure communicated by the fluid causes the caliper piston to push the pads against the disc brake, generating friction. Kinetic energy (which accumulates in the vehicle owing to speed) is transformed into heat owing to the friction between the disc and the pad, slowing down the vehicle.

During vehicle movement, which is often accompanied by several brakes, a large amount of heat accumulates on the vehicle brake discs, causing their temperature to increase. If the cooling performance of the braking system cannot maintain the temperature of the brake discs within a temperature range that ensures that the braking performance is not significantly affected, instability in the braking system and even safety problems may arise. If the braking system overheats, braking performance can deteriorate. Eventual premature failure can be caused by a number of factors, for example, (1) reduced coefficient of friction between the rotor and stator [1], (2) jitter due to excessive thermal distortion [2–3], (3) surface cracking due to high thermal stress on the metal rotor surfaces, (4) reduced mechanical strength and other performance changes of the brake disc, (5) increased wear of frictional materials, and (6) evaporation of brake fluid in the brake hydraulic cylinder [4]. Owing to the limitation of battery energy density, the only way to enhance the range of electric vehicles at this stage is by increasing the battery size, which leads to a greater weight of electric vehicles compared with that of traditional energy vehicles.

Under the same braking conditions, more heat will accumulate on the brake discs of electric vehicles because of their larger mass [5]; thus, the requirements of electric vehicles regarding the cooling performance of brake discs are more demanding. With the increasing popularity of electric vehicles in recent years, it has become essential to study ways to improve the cooling performance of brake discs. According to studies on the distribution of road traffic accidents caused by sudden failure of vehicle systems, braking systems have the greatest impact, with a proportion ranging from 32% to 50% [6–7]. Data from the fatal analysis reporting system (FARS) from 2010 to 2014 show that 6.35% of fatal accidents were caused by design or manufacturing defects in vehicles, and the principal vehicle defects were related to airbags, braking systems, seat belts, and speed control. Therefore, the performance of the braking system is particularly important for vehicles. In the braking system, car brakes are an important factor that affect the overall braking performance of the car and have a significant influence on its safety. The improvement in safety performance of car driving is mainly reflected in

* Corresponding author.
E-mail address: mxr2000@hanyang.ac.kr (H.-I. Yang).

https://doi.org/10.1016/j.aej.2023.08.035
Received 26 December 2022; Received in revised form 3 June 2023; Accepted 12 August 2023
Available online 22 August 2023

Fig. 1. Disc brake.

the improvement in the braking performance of the vehicle. Therefore, an accurate simulation of the disc brake cooling performance is essential for disc brake shape optimization, and many scholars have made improvements in this area. For example, Liu [8] obtained the transient temperature and stress field distributions under emergency braking and continuous braking. The disc bracket was optimized using the height, number, and angle of the ventilation slots as variables. Li [9] carried out structural optimization of the disc brake with a thermal structural ductility analysis of the disc brake during emergency braking, identified the areas where disc brake hotspots are likely to occur, and analyzed the finite element results. Belhocine et al.[10] studied the temperature changes in ventilated and solid discs under constant braking conditions and concluded that ventilated discs outperformed solid discs in terms of heat dissipation. Furthermore, the finite element results were analyzed to identify areas where hotspots tended to occur in the disc during braking. Qian [11] used computational fluid dynamics (CFD) and design of experiments (DOE) studies to optimize the shape and number of DC vanes to achieve maximum cooling performance. Sectors containing vanes with periodic boundary conditions were investigated because of their axisymmetric disc structure. Using three blade shape parameters, it was concluded that the number of vanes, leading-edge radius, blade length ratio, and taper length sequentially improved the cooling performance. Although these methods are effective, the results exhibit poor stability and long response times. To improve the various properties of brake discs, many analyses of brake discs have been performed using thermal structural ductility analysis or CFD to obtain optimized models. However, the effects of the number, shape, and thickness of ventilated disc vanes on the performance of brake discs have been under-researched.

According to the literature, the best cooling method for brake disc pads is convection [28]. Consequently, vented discs are now utilized in cars to enhance convection cooling. Two parallel friction surfaces are joined using a string of radial vanes or pins to form a vented disc, which has a larger cooling surface than a solid disc. Moreover, a vented disc functions as a centrifugal fan, drawing nearby cold air into the channels of the disc and allowing it to pass through, thereby dissipating the generated heat. To reflect the material property values with temperature and the stresses acting on the disc brake over time, a finite element model based on the contact analysis theory was created for this study. The output of the model was then analyzed. By calculating the heat flow rate, speed, and convective heat transfer coefficient generated during emergency braking, the loads were determined for the design and optimization of the disc brake. The braking performance was improved by varying the shape, number, distribution, and ventilation gap (thickness) of the vanes. Using the UDF function, a heat flux was applied to the brake disc with time, and then, using a CFD method (the software used was Fluent 2020R2), a heat dissipation analysis was carried out to evaluate the cooling performance of different brake discs and obtain an optimized model.

This paper contributes as follows:

(1) Regardless of the braking that may occur during wheel locking, the wheels perform only a pure rolling action.
(2) A braking pressure is applied to the bottom of the friction pad. The disc brakes are composed of isotropic elastic materials.
(3) The initial temperature of the vehicle's front wheel disc brakes is 80 °C and is maintained at a uniform temperature.

2. Related work

Regarding the improvement in the cooling effect of the ventilation tray, recently, many scholars have also carried out a significant amount of research. For example, Coulibaly et al. [12] showed that the maximum temperature of the ventilated disc is approximately 47° C lower than that of the solid disc at different ambient temperatures. Vdovin et al. [13] studied the aerodynamics of a complete vehicle and calculated the convection and radiant heat transfer. The internal convection of the brake disc was calculated as 53% of the total convection of the brake disc. Dubale et al. [14] studied the differences between the thermometric mechanical properties of drilled, slotted, and solid disc brake profiles. They noted that grooved brake discs showed the best performance, and it was also observed that as the number of vents in the disc brake rotor increased, the heat dissipation also increased. However, neither the relationship between stress and deformation nor the change with the increase in the number of holes was mentioned. Yan et al. [15] investigated the effect of cross-drilled holes on ventilated brake discs. Simulations were performed on some of the discs, and the results indicated an improvement in the overall cooling performance of 22% to 27%. In a downhill experiment, the temperature of the cross-drilled disc was 141 °C lower than that of the undrilled disc.

Qiu et al. [16] studied the heat distribution ratio between the brake disc and pad at high thermal contact conductivity and found that the heat from the disc and pad accounted for 95% and 5% of the total heat, respectively. Hong et al. [17] added circular friction blocks to a brake disc to reduce the temperature and thermal stress on the disc and used the Taguchi design method to derive reductions in maximum temperature, temperature gradient, and thermal stress of 16.8%, 55.2%, and 11.2%, respectively, for a disc using optimized bedding. Jafari et al. [18] considered all the braking components used in a normal car, including the tires and dust cover. The results indicated that the heat transfer over the internal vanes of the brake disc during cooling was between 58% and 71% of the total convective heat transfer. Garcia-Leon et al. (who studied the changes in shape with vanes) proposed a new geometric arrangement. The airflow of the vehicle disc brakes was improved through CFD analysis by means of ventilation vanes based on the aerodynamic profile considerations of NACA 66–209, which in turn led to the model with the best cooling performance. Topouris et al. [19] compared a ventilated disc with radial vanes, two ventilated discs with curved vanes, and a solid disc. Experiments on a specially designed spin platform showed that a ventilated disc with radial vanes had the highest convective heat dissipation, with a 30% improvement compared to that of a solid disc. Park et al. [20] conducted a study to improve the heat-transfer rate of a ventilated disc brake. The surface geometry of the disc brake flow path was modified from smooth to a spiral groove. The numerical analysis showed that the local Nusselt number decreased monotonically with the distance between the wave crest and spiral groove. This suggests that the increase in surface area provided by the spiral groove geometry improved the recirculation behavior of the airflow and the formation of vortices.

Duzgun [21] used finite element analysis (FEA) to model three different ventilated disc brakes and investigate their thermal structural behavior. The FEA results show that different rib shapes reduce the heat generation on the solid surface of the brake disc by up to 24%. The experimental study of the dissipation of heat generated on the surface of the disc was verified by the FEA, and was found to be in the range of 1.13%–10.87% for the temperature analysis. This improves the braking performance so that the coefficient of friction between the brake pad and the brake disc surface does not change significantly, which would threaten the driving safety. Thus, the surface wear of the brake pads remains within manageable limits, especially under continuous braking conditions. Belhocine and Afzal [22] conducted transient thermal analyses of ventilated and solid brake discs. Using a finite-element approach, it was concluded that the materials used in the brake disc must have low thermal conductivity during the braking process, thus generating a large thermal gradient and increasing the surface temperature of the disc brake. The results showed that brake discs made from FG15 were cooler than those made from FG20 and FG25AL. Therefore, the most suitable material for brake discs is FG15 gray cast iron because it has the best thermal properties. Lakkam et al. [23] investigated the temperature gradient of a disc brake to assess its thermal convection coefficient (h) using experimental and numerical tests. The value of h was corrected by varying the temperature distribution of the disc brake under steady-state forced thermal convection conditions. The distribution and dissipation of heat transfer were investigated using numerical and finite element calculations and verified experimentally. Modanloo [24] analyzed and simulated the thermal behavior of a high-speed brake disc. Forced convection was applied to the inner surface to simulate ventilation. The temperature gradient in the direction of disc thickness was higher in the ventilated disc than in the solid disc. In addition, the maximum temperature of a ventilated disc was reduced to 659 °C compared with 782 °C for a solid disc. Yan et al. [25] introduced a new heat-dissipation medium to replace ventilated vanes. Compared to finned discs, it not only reduced the disc temperature by 16%–36%, but also resulted in a more uniform heat transfer. Afzal and Mujeebu [26] simulated the thermal performance of brake discs with different configurations using a uniform convective heat transfer coefficient. The results indicated that replacing straight vents with curved vents improved the thermal performance of the discs. Kumar et al. [27] simulated the temperature distribution of three solid discs and demonstrated that drilled and slotted discs exhibited high heat fluxes and lower temperatures.

Although these studies are effective in improving the cooling effect of ventilated discs, the obtained stability and robustness are poor. The scheme in this study effectively remedies the shortcomings of these schemes.

Table 1
Values of thermal conductivity and specific heat capacity of grey cast iron.

Temperature [℃]	Poisson's ratio	Thermal conductivity [W/m•℃]	Specific heat [J/kg•K]
0	0.25	53.3	457
20	0.25	53.1	460
100	0.256	52.5	474
200	0.263	51.0	488
300	0.27	49.5	502
400	0.275	49.0	516
500	0.279	48.0	530

Table 2
Design parameters and interval levels.

Variable Level		1	2	3
1	Ventilation gap (mm)	10	12	14
2	Vane angle (°)	29	37	45
3	Vane number	30	36	42

Table 3
DOE L9(3^3) Orthogonal arrays for three factors and three levels.

$L3^3$	Ventilation gap (mm)	Vane angle (°)	Vane number
1	10	29	30
2	10	37	36
3	10	45	42
4	12	29	36
5	12	37	42
6	12	45	30
7	14	29	42
8	14	37	30
9	14	45	36

3. Studied configuration

The material used for the disc brake must have a low thermal conductivity during the braking operation to produce a large thermal gradient and increase the disc brake surface temperature. The brake disc can cool faster because of the more rapid heat exchange between the surface and air. Grey cast iron (GCI), which has great thermal conductivity, outstanding corrosion strength, low noise, low weight, long life, steady friction, low wear rate, and excellent longevity, as well as good castability, machinability, and affordability, is the best material for brake discs. Disc brakes assume that the friction contact interface is an ideal plane and that friction follows Coulomb's law. The instantaneous temperature of the disc brake during braking was assumed to be equal to the maximum temperature at that point in the contact zone. The effect of the radiative heat transfer was ignored in this study. The ambient temperature was maintained at a constant value during braking.

Many light alloys have been tested as gray cast iron substitutes; however, their high cost prevents their extensive use. The thermal conductivity and specific heat capacity of gray cast iron as a function of temperature are presented in Table 1 [29]. A new material was formed by inserting the data from Table 1 into the CFD procedure.

All the components of the brake disc were assumed to be composed

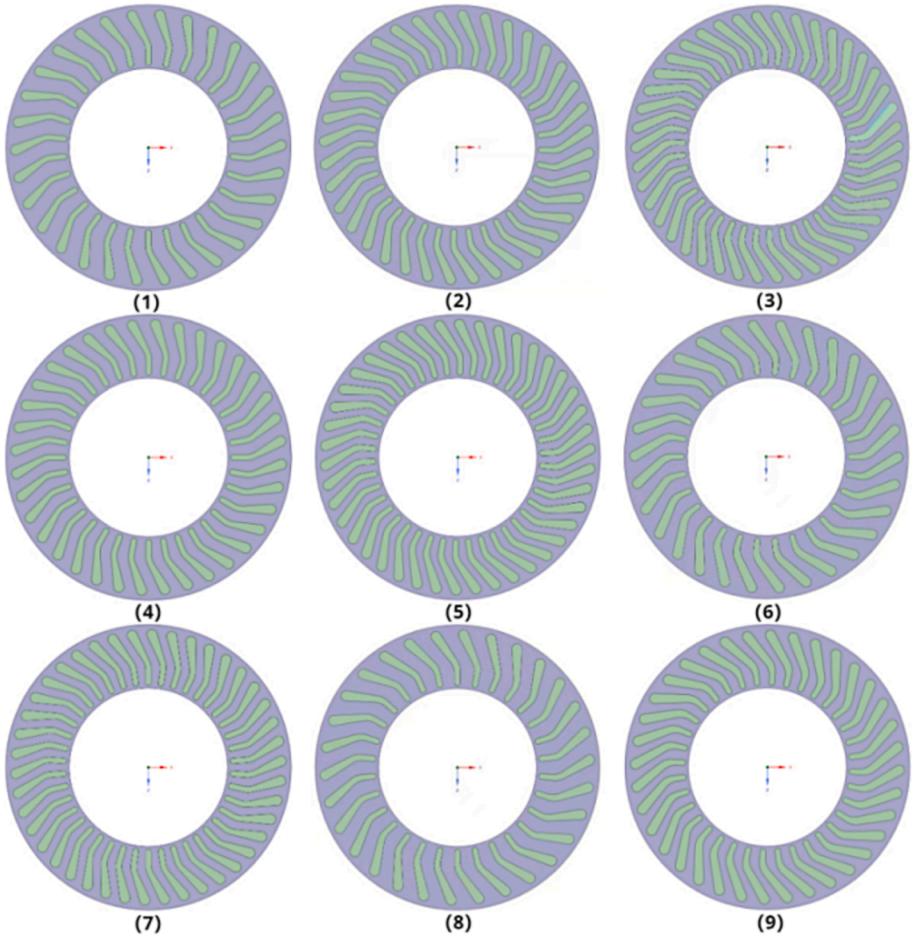

Fig. 2. Cross sectional view of the Taguchi L9 design for radial ventilated brake disc.

Table 4
Number of grids for step 1 and step 2.

Model	Step 1	Step 2
1	1,630,182	1,729,228
2	1,639,819	1,743,417
3	1,632,998	1,733,759
4	1,654,945	1,768,840
5	1,657,242	1,786,913
6	1,649,840	1,763,739
7	1,687,137	1,799,454
8	1,684,291	1,773,266
9	1,684,374	1,779,539

of gray cast iron for simplicity in the calculation. The model measurements were derived from the brake disc of a small SUV. All brake discs were modeled such that the number of vanes, steering angle, and ventilation clearance could be altered without affecting the size of the disc to maintain the same variables (see Tables 1, 2, and 3 and Fig. 2).

It can be observed from Fig. 2 that orthogonal arrays are arrays that can be designed so that the factor levels have equivalent weights, thus allowing each factor to be evaluated independently of all other factors. The ability to evaluate multiple factors independently without interaction makes it possible to process a large number of experiments and obtain results at once [30]. In the simulation, three parameters were set to improve the thermal performance of disc brakes. Three factor levels were used for each parameter, requiring 27 analyses; however, only nine analyses were performed using an orthogonal alignment table. An orthogonal alignment table was prepared. The figure shows the intermediate cross-section of each group of models (see Table 4).

Table 5
Grid Sensitivity Test.

Number of grids	Temperature after cooling (℃)
875,321	147.67
1,630,182	137.14
3,327,890	137.26

As shown in Table 5 that we did a grid sensitivity test. Modell was tested on 87,521 grids, 16,308 grids, and33278grids, and the calculation results were consistent between 16,308 grids and33278grids, so in order to save calculation time this paper uses 16,308 grids for cfdcalculation.

As can be observed from Figs. 3 and 4, the simulation was divided into two steps. First, the velocity and pressure distributions were calculated using the SST k-omega turbulence model.

The k–omega equation based on the SST model considers the transport of the flow shear stress and can accurately predict fluid separation at the onset of flow and under negative pressure gradients. The greatest advantage of the SST model is that it considers the turbulent shear stress and thus does not overpredict the vortex viscosity. The flow kinetic energy equation for the SST model is given by Eq. (1), and the specific dissipation rate transport equation is as follows:

$$\rho\frac{D\omega}{Dt}+\rho\frac{\partial(\omega u_i)}{\partial x_i}=\frac{\partial}{\partial x_j}\left(T_\omega\frac{\partial\omega}{\partial x_j}\right)+G_\omega-Y_\omega+D_\omega \tag{1}$$

where D_ω represents the orthogonal dispersion term, and the remaining parameters have the same meaning as those in the standard k-omega model.

The parameters of the SST model are set as listed in Table 6.

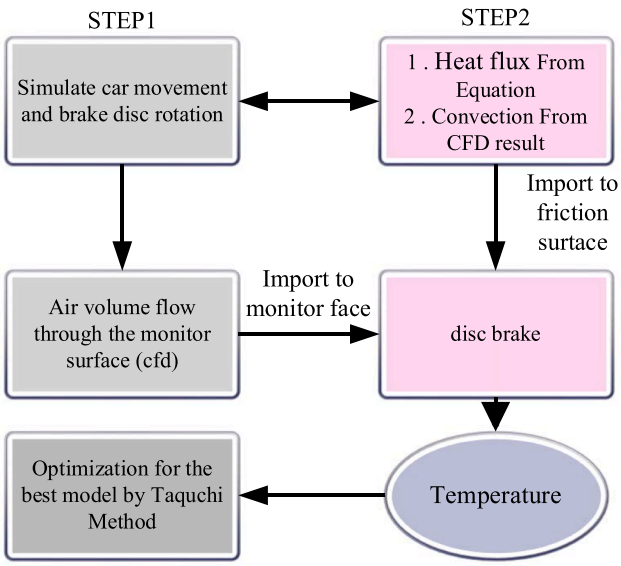

Fig. 3. Flowchart of the simulation process.

While the disc rotated with the vehicle (at a speed of 60 km/h), a monitoring surface was also provided between each of the disc's vanes to track the volume flow rate via each surface. For each model, a graph of the volumetric flow of air through the monitoring surface was obtained, and the stabilized portion was averaged. The middle portion of the brake disc's velocity distribution and the volumetric flow velocity via the monitoring surface were determined by transient analysis, and velocity clouds were created for each model's middle section to accelerate the simulation. The volumetric flow rate passed through was then imported into the second step of the simulation process and the heat flux during braking (the car decelerated from 100 km/h, at a deceleration rate of 0.5 g, to 0 km/h in 5.663 s) was calculated and input using Eq. (1). In the second step only the heat convection process was calculated, first importing the decreasing heat flux in the time between 0 and 5.663 s. The cooling process of the brake disc was calculated from 5.663 to 100 s by introducing a directional air flow, and the disc was not considered to rotate in the second step. The temperature of the brake disc after the cooling process was obtained by transient analysis and the maximum temperature difference during the simulation was obtained. Table 6 presents the speed of the car as a function of time during the simulation (see Fig. 5 and Table 6), and the heat flux on the brake disc surface was equal to $1102721 - \text{time} \times 194723.8$ (Kw/m^2).

Fig. 6 shows the calculation domain and boundary conditions. The meshes used in this study were unstructured tetrahedral. The rotational

Table 6
Parameter settings.

Average speed	50	m/s
Medium density	1.225	Kg/m^3
Dynamic viscosity	1.7894e − 5	Kg/(m.s)
Characteristic length	0.004	m
Turbulent kinetic energy		8.87476e + 0 m^2/s^2
Turbulence intensity		4.86478%
Turbulence length scale		1.70403e − 3 m
Turbulent kinetic energy dissipation rate		1.55152e + 4 m^2/s^3
Turbulent Viscosity Ratio		25.53258
Specific dissipation rate		23795.541281/s

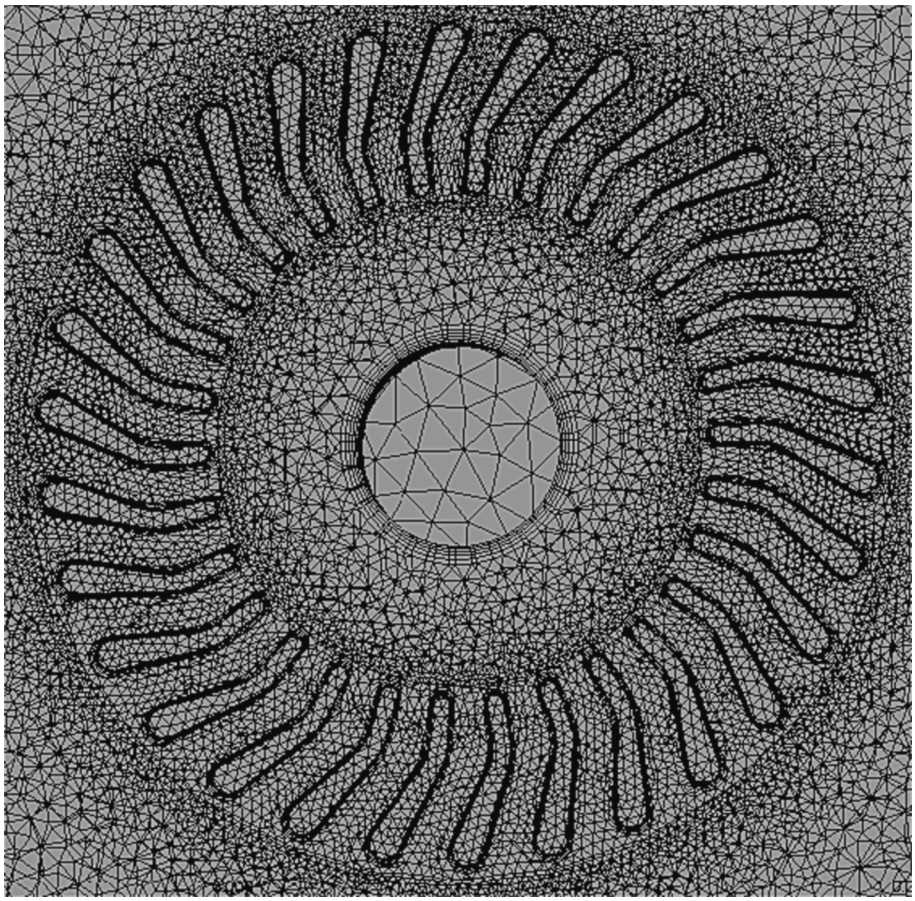

Fig. 4. Mesh.

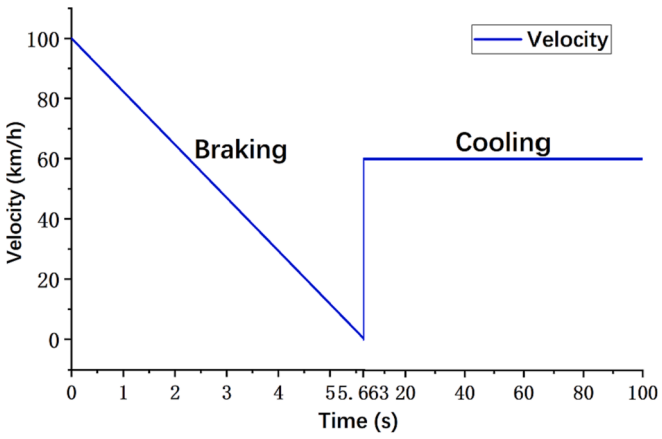

Fig. 5. Velocity change in the emergency braking and cooling analysis.

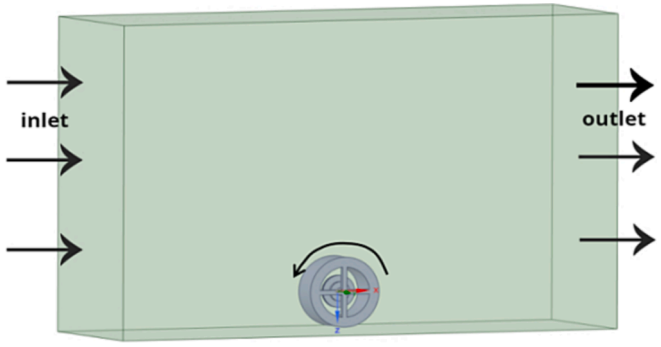

Fig. 6. Motion track.

Table 7
Velocity change in the emergency braking.

100–0 km/h	Symbol	Value	Unit
Maximum Velocity of Vehicle	V_{max}	100	km/h
Minimum Velocity of Vehicle	V_{min}	0	km/h
Deceleration	a_d	0.5 g	m/s^2
Time for Decelerating	t_d	5.663	s

Table 8
Initial and boundary conditions of the domain.

Parameter	Value
Inlet velocity	16.667 m/s
Outlet pressure	1 atm
Initial temperature of the domain	26 ℃
Initial temperature of the disc and pads	80 ℃
Angular velocity of the disc and pads	60 rad/s

speed of the pad and brake disc was 60 rad/s. The size of the fluid domain was 2 m * 0.8 m * 1.5 m, which was sufficient to simulate the air flow around the tires when the car was moving. The convective heat exchange between the brake disc and surrounding airflow was considered. Air entered the fluid domain instead of the car, and the boundary conditions of the inlet are listed in Table 7. The airflow entered the area from the entrance, passed through the channel, and left the area through the exit. The rotational motion of the tires, rims, and brake discs is proportional to the speed of the car. To reduce calculation time and complexity, parts that have little effect on air flow were removed from the model, and only the rotation of tires, wheels, and brake discs were simulated. An inlet speed of 100 km/h (16.667 m/s) and outlet pressure were used (Table 8) [34,35]. Sliding wall boundary conditions were assigned to the side and upper walls to reduce their effects on airflow. This method provides a good simulation of the car motion and rotation of the brake disc with the car motion (see Fig. 7).

The airflow velocity was significantly influenced by the steering angle of the vanes of the disc, with the effect being the highest at a steering angle of 37°, as can be observed in the velocity cloud diagram of the middle cross-section of the brake disc (Fig. 8). Given that all three variables can affect the volumetric flow rate past the monitoring surface, the influence of the number of vanes on the airflow velocity is ambiguous and thus needs to be examined further (see Fig. 9).

As shown in Table 9, the ventilation gap has the greatest effect on the volumetric flow rate of the monitoring surface, which also plays a decisive role in the heat dissipation in the next step.

The well-known Navier-Stokes equations for k-∈ turbulent model are solved to describe the velocity and pressure fields for the computational domain as

$$\rho\nabla\cdot(\boldsymbol{u}) = 0 \tag{2}$$

$$\rho(\boldsymbol{u}\cdot\nabla)\boldsymbol{u} = \nabla\cdot\left[-p\boldsymbol{I} + (\mu+\mu_T)\left(\nabla\boldsymbol{u} + (\nabla\boldsymbol{u})^T\right)\right] \tag{3}$$

$$\rho(\boldsymbol{u}\cdot\nabla)k = \nabla\cdot\left[\left(\mu+\frac{\mu_T}{\sigma_k}\right)\nabla k\right] + \mu_T\left[\nabla\boldsymbol{u}:\left(\nabla\boldsymbol{u} + (\nabla\boldsymbol{u})^T\right)\right] - \rho\varepsilon \tag{4}$$

$$\rho(\boldsymbol{u}\cdot\nabla)\varepsilon = \nabla\cdot\left[\left(\mu+\frac{\mu_T}{\sigma_\varepsilon}\right)\nabla\varepsilon\right] + C_{\varepsilon1}\frac{\varepsilon}{k}\mu_T\left[\nabla\boldsymbol{u}:\left(\nabla\boldsymbol{u} + (\nabla\boldsymbol{u})^T\right)\right] - C_{\varepsilon2}\rho\frac{\varepsilon^2}{k} \tag{5}$$

The energy equation is used to simulate the temperature distribution for 3D Cartesian coordinate as

$$\rho C_p\frac{\partial T}{\partial t} + \rho C_p\boldsymbol{u}\cdot\nabla T - \nabla\cdot(k\nabla T) = Q \tag{6}$$

When the vehicle is traveling at a stable speed, given its mass m_v and speed V, the kinetic energy can be expressed as:

$$KE = \frac{1}{2}m_v V^2 \tag{7}$$

So when the vehicle decelerates from V_1 to V_2, the energy consumed during the braking process is:

$$KE = \left(\frac{1}{2}m_v V_1^2\right) - \left(\frac{1}{2}m_v V_2^2\right) \tag{8}$$

However, it is also necessary to consider the rotational inertia of transmission system components, which increase kinetic energy. Given the inertia I_D and angular velocity ω of the component, this portion of kinetic energy is represented as:

$$KE_I = \left(\frac{1}{2}I_D\omega_1^2\right) - \left(\frac{1}{2}I_D\omega_2^2\right) \tag{9}$$

The total kinetic energy is

$$KE_T = \left(\left(\frac{1}{2}m_v V_1^2\right) - \left(\frac{1}{2}m_v V_2^2\right)\right) + \left(\left(\frac{1}{2}I_D\omega_1^2\right) - \left(\frac{1}{2}I_D\omega_2^2\right)\right) \tag{10}$$

Due to the unavailability of inertia data for rotating components, a constant k was used. Listen to Bryant's suggestion [31], and for the simulation conducted in this article, take the value of k as 1.

When the deceleration is constant, the average braking power P_b is equal to the ratio of kinetic energy KE_T to stopping time t_s

$$P_b = \frac{KE_T}{t_s} \tag{11}$$

The proportion of braking force acting on the front axle is x_f, and the braking power on one side of a front rotor can be expressed as P_{bf}

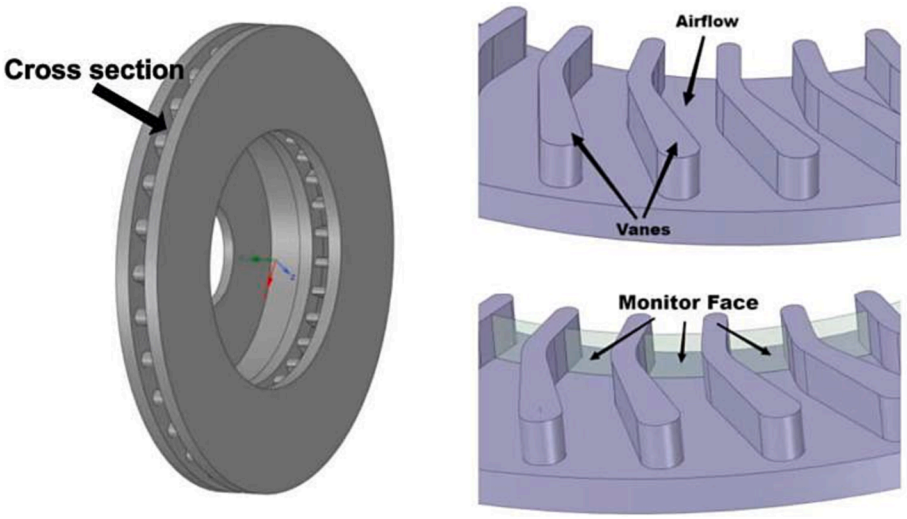

Fig. 7. Set up of a monitoring surface between the vanes of the brake disc to obtain the volume flow rate across the monitoring surface.

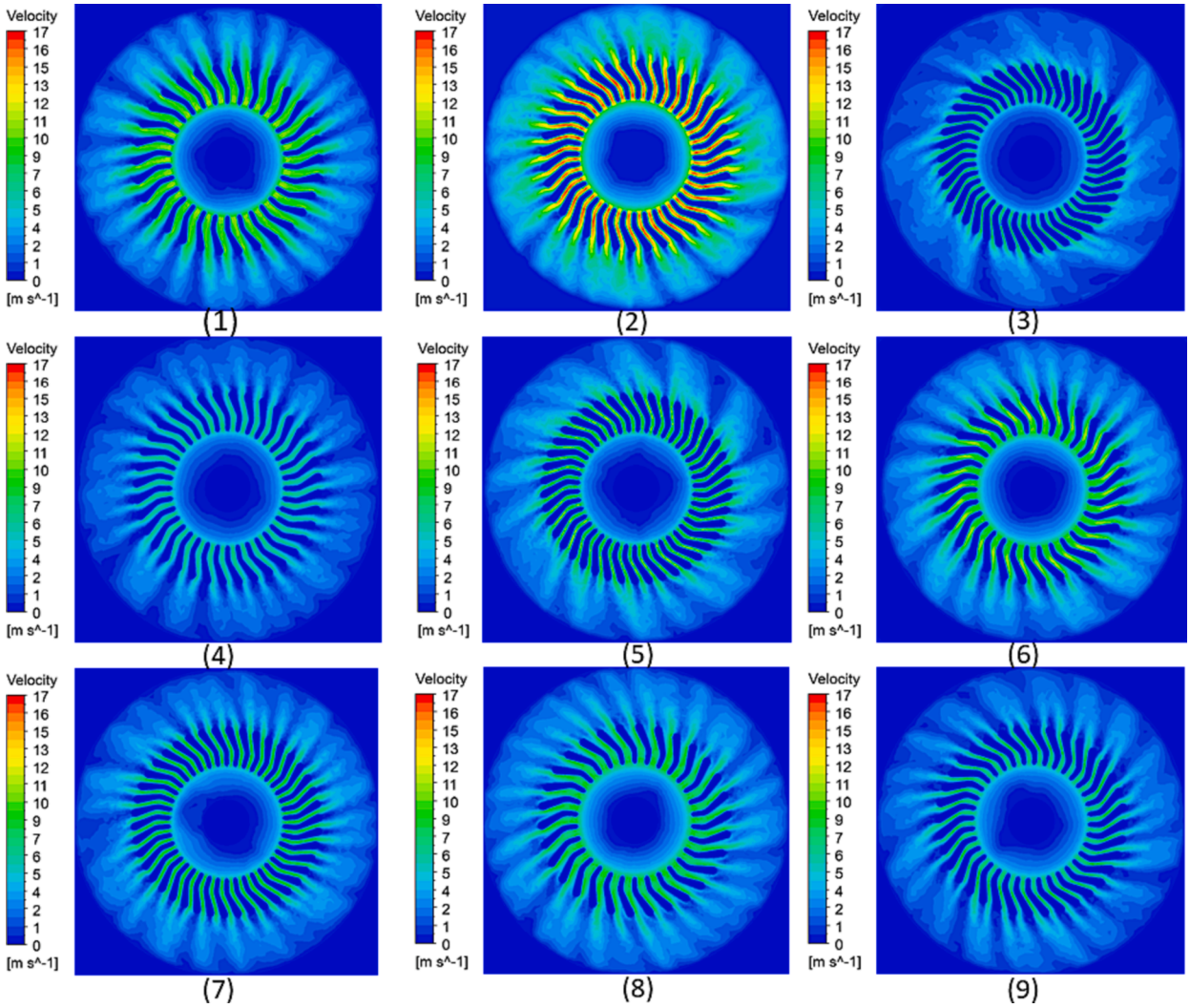

Fig. 8. Velocity distribution of the middle cross section of brake disc.

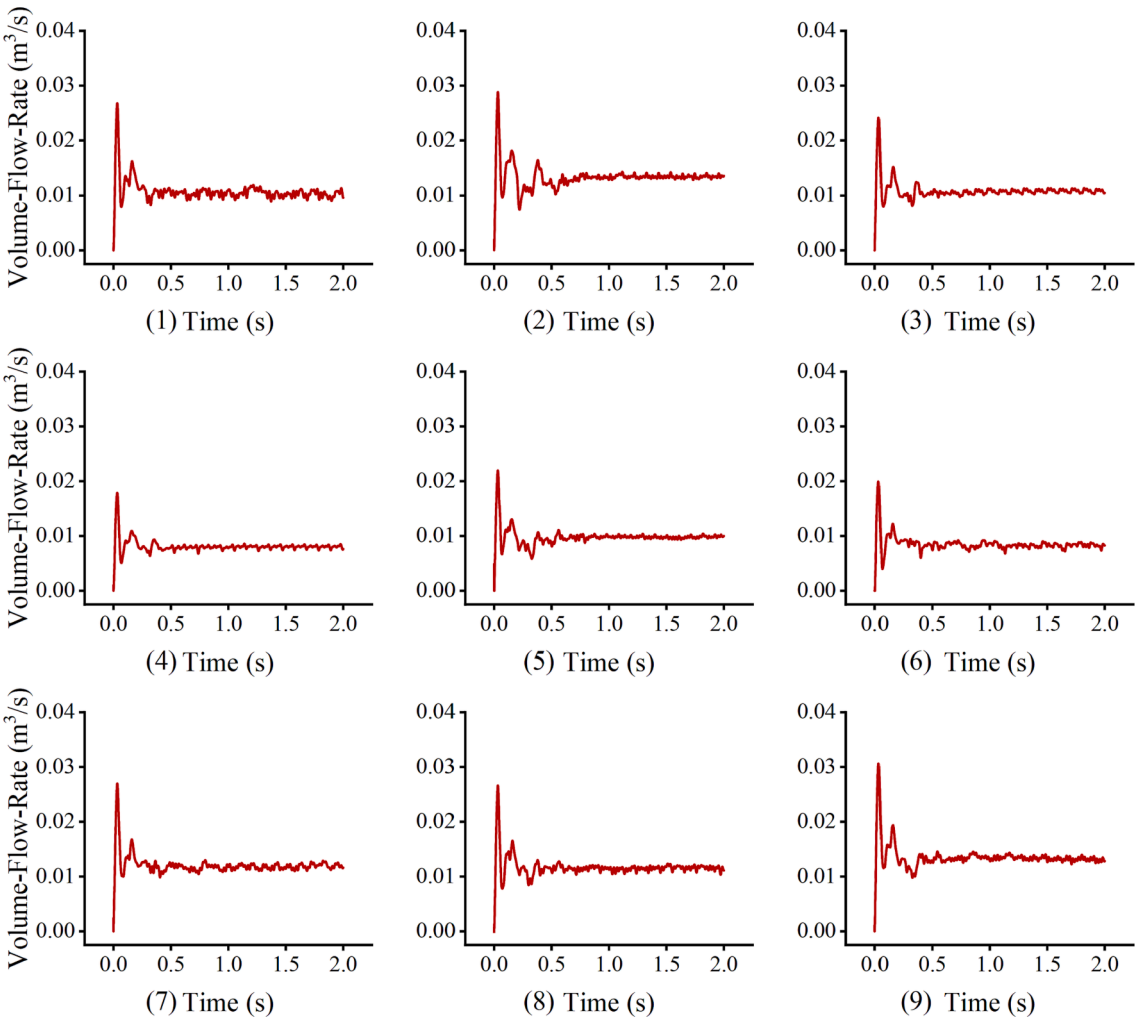

Fig. 9. Volume velocity diagram of monitoring surface.

Table 9
Volume flow rate across the monitoring surface for each model.

NO	Average Volume Flow Rate (m^3/s)
1	0.010378057829
2	0.010807989317
3	0.008024563916
4	0.009806321282
5	0.008265661186
6	0.011833464403
7	0.011499608247
8	0.013295819824
9	0.013470219039

$$P_{bf} = P_b \times x_f \times 0.5 \times 0.5 \tag{12}$$

Given that the surface area on one side of the brake disc is A_D, the heat flux on one side can be expressed as

$$\dot{q} = \frac{P_{bf}}{A_D}$$

In order to calculate the heat flux, the coasting deceleration value of the vehicle was used, which takes into account the transmission resistance and rolling resistance. Therefore, a constant of 0.07 g was used, called r_r. Using the coasting deceleration value, the proportion of vehicle deceleration caused by the brake was obtained. Then use it to calculate heat flux.

Table 10
Constant values.

Variable	Value
m_v[kg]	1900
k[-]	1
x_f[-]	0.72
η_d[-]	0.99
A_D[m^2]	0.0328
r_r[m/s^2]	0.07 g

The study performed by Tirovic [31] showed that the heat generated during braking was dispersed between the brake pads and discs in a ratio of 1 to 99. However, research by Day and Newcomb [32] has shown changes in the interface pressure distribution due to wear and thermal expansion, resulting in temperature changes between the disc brake and brake pad. To simplify this study, a constant value was used for η_d, based on Tirovic's [31] study, resulting in a value of 0.99. For a single-disc brake on the front axle of a vehicle, the equation for calculating the instantaneous heat flow rate is given by Eq. (14).

$$\dot{q}_n = \frac{[0.125 m_v k (V_n^2 - V_{n+1}^2) x_f \eta_d]}{(t_{n+1} - t_n) A_D} \times (1 - \frac{r_r}{a_d}) \tag{14}$$

Table 10 lists the data for the car and the values of the constants in the formula. The above equation calculates the maximum heat flux during braking to be 1102 Kw/m^2. The heat flux was fed into the friction

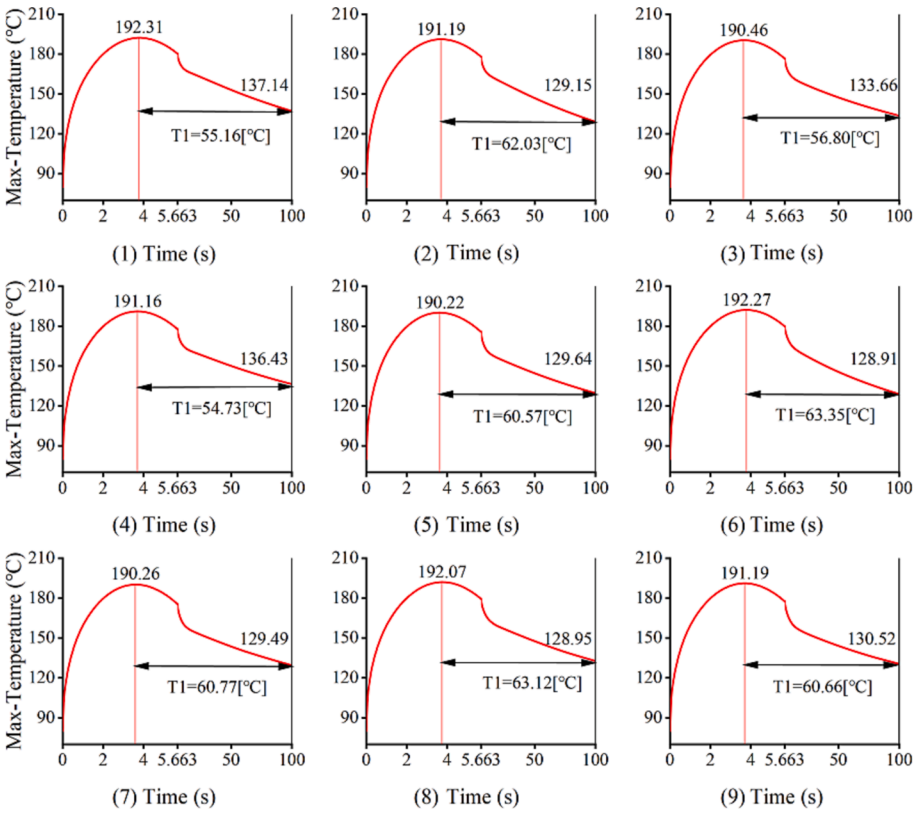

Fig. 10. Temperature profiles for each model (0–100 s).

surface of the brake disc via the UDF function (linearly decreasing from 0 to 5.663 s) and the heat was dissipated by maintaining a speed of 60 km/h at the end of braking to obtain the temperature of the brake disc after 100 s [32,36,37]. The temperature obtained was the temperature of the brake disc after 5.663 s of braking process (the braking process also includes the heat dissipation process) and 100 s of heat dissipation process. The graphs of the temperature profiles from 0 to 100 s for each model show that during the braking process of the car (0 to 5.663 s), the temperature did not increase continuously, but started to decrease slowly after a maximum value. This occurred because the heat flux decreased over the period from 0 to 5.663 s. The braking process was also accompanied by heat transfer from the various parts of the brake disc and convective heat exchange with the air (see Fig. 10).

Cooling performance is a property where the greater value is the better; therefore, the signal-to-noise (SN) ratio was calculated using the following formula:

The SN ratio was calculated from the results of a cooling analysis of the emergency brake. The temperature difference is characterized by the SN ratio calculation, and the results of the analysis of the nine models and their influence on the design parameters are plotted along with the optimization factor. The x-axis coordinates are the ventilation gap and steering angle of the ribs, and the number of ribs and y-axis coordinates are the SN ratios (see Fig. 11). The higher the SN ratio of the temperature difference expressed by the larger-the-better characteristics for each design variable, the better are the expressed characteristics.

$$SN = -10\log_{10}\frac{1}{10}\sum_{i=1}^{n}\frac{y_i^2}{n} \tag{15}$$

The black lines represent case 1, grey lines represent case 2, light grey lines represent case 3, and dashed lines represent the simulation results to which the failure strain of the criterion was applied. The failure strains calculated by the criterion are listed in Table 10, where h is the height of the mesh and b is the width of the mesh [33]. As shown in these figures, the simulation results before applying the criterion show a significant mesh dependency. According to the mesh size, the HJC model had a difference of 201 m/s in the simulation results, the CSC model had a difference of 198 m/s, and the K&C model had a difference of 239 m/s. The reliability of the simulation results cannot be confirmed using these values. When the failure strain determined by the criterion was applied to the concrete plate in the FEA, the variation in the simulation results decreased significantly. As indicated by the dashed lines in Figs. 6, 7, and 8, the difference in the residual velocity was reduced. Subsequently, the criterion was applied to the concrete plate presented in Table 11.

4. Results

A data analysis of the cooling performance of a ventilated brake disc was performed. The heat flux generated during the braking process was calculated using Eq. (16). The heat flux was fed into the friction surface of the brake disc using a UDF function. The change in temperature after 100 s of heat dissipation was calculated using CFD. The effects of the three parameters on the cooling performance of the ventilated disc were evaluated using Taguchi's L9 design, the S/N ratio, and linear regression prediction methods. Based on the analysis, we obtained the following results:

The volume flow of air and heat exchange area were increased by increasing the ventilation gap from 10 to 14 mm, enhancing the heat dissipation capacity on the disc and increasing the temperature difference between 0 and 100 s.

The angle of the vanes had the greatest influence on the heat dissipation capacity of the disc, increasing the heat transfer from 0° to 37°, but not as much at 45° as at 37°.

The number of vanes was 30, which provided the best cooling effect on the disc.

The effect of each parameter on the cooling performance of the disc was in the following order: angle of vanes > ventilation gap > number of

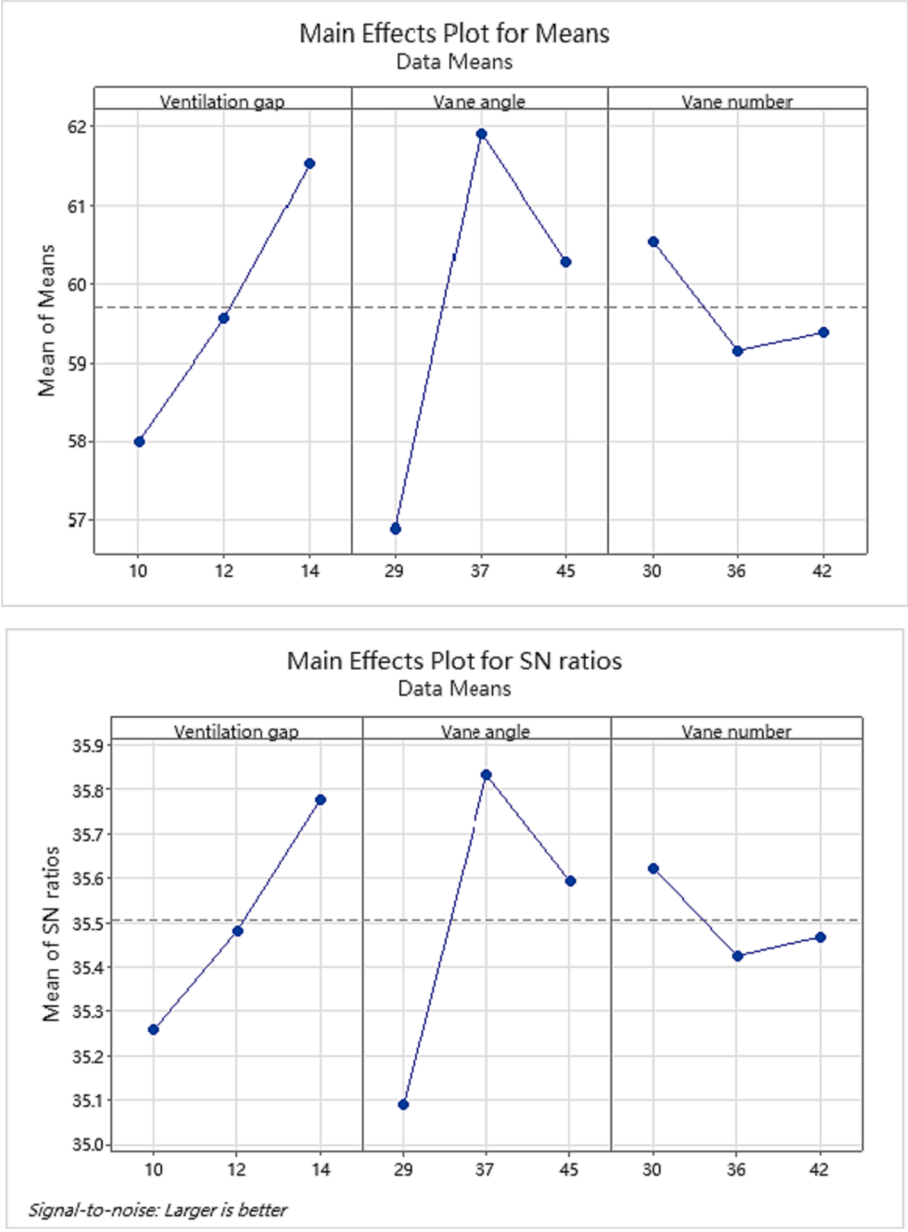

Fig. 11. Optimization factors legend.

Table 11
Failure strain calculated by the criterion of mesh.

B (mm)	Case 1 (h = 35.5 mm)	Case 2 (h = 18.8 mm)	Case 3 (h = 7.22 mm)
3.04	0.0365	0.0425	0.0458
4.08	0.0364	0.0425	0.0456
6.21	0.032	0.0399	0.0458
8.72	0.01335	0.01558	0.0174
12.3	0.00548	0.005898	0.00635
20.4	0.00188	0.001874	0.00235

vanes.

The model with the highest cooling capacity was predicted using the Taguchi correlation presented in Table 12.

$$y = \beta_0 + \beta_1 x_1 + \beta_2 x_2 + \ldots \beta_k x_k + \varepsilon \quad (16)$$

Linear regression is an analysis method in mathematical statistics

Table 12
Taguchi L9 design for the ventilated brake disc and temperature change results.

NO	Ventilation gap (mm)	Vane angle (°)	Vane number	**ΔT** (℃)
1	10	29	30	55.16
2	10	37	36	62.03
3	10	45	42	56.79
4	12	29	36	54.72
5	12	37	42	60.57
6	12	45	30	63.34
7	14	29	42	60.75
8	14	37	30	63.12
9	14	45	36	60.66

that uses regression analysis to determine quantitative relationships between two or more variables. With the independent and dependent variables, the relationship between the two variables can be approximated by a straight line, predicting the value of the dependent variable. When there is one independent variable and one dependent variable, it

Table 13
Design parameters for the optimized ventilated brake disc.

Ventilation gap (mm)	Vane angle (°)	Vane number	**ΔT** (℃)
14	37	30	64.59

is called univariate linear regression analysis. When two or more independent variables are included and the relationship between the dependent and independent variables is linear, it is called multiple linear regression analysis. In general, linear regression allows the equation to be found using least squares and the line y = ax + b to be calculated [33,38,39]. In general, there is often more than one factor that affects y. Assuming the factors X_1,X_2,…, X_K, the following linear relationship can generally be considered:

$$y = \beta_0 + \beta_1 x_1 + \beta_2 x_2 + \ldots \beta_k x_k + \varepsilon \quad (17)$$

$$\Delta T = 44.8 + 0.879 \text{ ventilation gap} + 0.212 \text{ Vane angle} - 0.097 \text{ Vane number} \quad (5)$$

Using this linear equation, the brake disc model with the best cooling performance can be predicted, and subsequent studies can be conducted without being limited to the three parallels of the three variables in this study.

Table 13 presents the brake disc model with the best cooling performance and its parameters obtained by Taguchi's predictions. After the braking process and cooling up to 100 s, the optimized maximum temperature reduction is 64.59 °C.

5. Conclusion

Through the outer fan outlet of the brake system of a car, the air is blown into the brake system along the space between the rear disc of the fan and the fan cover by the action of the fan. Part of the air is obstructed by the end cap and cooling fins. This causes the air to decrease in speed after passing through the end cap and blow through the cooling fin air ditch at a lower speed to reach the other end, whereas the other part forms a disturbance at the fan.

Therefore, in this study, the experimental method of Taguchi design was used to optimize the design of a ventilated brake disc with radial vanes using three designs. For this reason, in this study, the experimental method of the Taguchi design was used to optimize the design of a ventilated brake disc with radial vanes using three design parameters (i.e., number of vanes, vane thickness, and steering angle), and the airflow and temperature distribution around the brake disc and tire were simulated using finite elements.

The future research direction of this study considers that the lowest airflow velocity occurs in the middle of the brake housing because the airflow moves laterally between the air grooves of the adjacent cooling fins in the middle of the housing. The obstruction of the airflow by the adjacent cooling fins is large, resulting in a sharp drop in airflow velocity. Therefore, more attention will be paid to the optimization of this part.

Declaration of Competing Interest

The authors declare that they have no known competing financial interests or personal relationships that could have appeared to influence the work reported in this paper.

References

[1] T.K. Kao, J.W. Richmond, A. Douarre, Brake disc hot spotting and thermal judder: an experimental and finite element study, Int. J. Veh. Des. 23 (2000) 276–296, https://doi.org/10.1504/ijvd.2000.001896.

[2] L. Augustins, F. Hild, R. Billardon, S. Boudevin, Experimental and numerical analysis of thermal striping in automotive brake discs, Fatig. Fract. Eng Materials and Structures 40 (2017) 267–276, https://doi.org/10.1111/ffe.12495.

[3] J.E. Hunter, S.S. Cartier, D.J. Temple, R.C. Mason, Brake fluid vaporization as a contributing factor in motor vehicle collisions, SAE Tech. Pap. (1998), https://doi.org/10.4271/980371.

[4] P. Grzes, W. Oliferuk, A. Adamowicz, K. Kochanowski, P. Wasilewski, A. A. Yevtushenko, The numerical-experimental scheme for the analysis of temperature field in a pad-disc braking system of a railway vehicle at single braking, Int. Commun. Heat Mass Tran. 75 (2016) 1–6, https://doi.org/10.1016/j.icheatmasstransfer.2016.03.017.

[5] Andrej, Z., & Natalya, K. (2017). Substantiation of the replacement interval of construction machines by the target reliability level.Architecture and Engineering, 2(1). Shtayts, E. (2014). Youth and Science: proceedings of the 10th All-Russian Scientific and Technical Conference of Students.

[6] Zubriski, S., Krasavin, P., & Ruzskiy, A. (2012). Formation of the system for monitoring of the technical condition of transportation vehicles admitted for operation according to road safety conditions.

[7] L. Yan, Thermal-structural Coupling Analysis and Structure Optimization of Passenger Car Disk Brake (Master's Thesis), Zhejiang Sci-Tech University, 2016.

[8] L.i. Fei, Finite Element Analysis and Optimization Design of Vehicle Ventilated Disc Brake (Master's Thesis), Shandong jian zhu University, 2019.

[9] R. Jafari, R. Akyüz, Optimization and thermal analysis of radial ventilated brake disc to enhance the cooling performance, Case Studies in Thermal Engineering 30 (2022), 101731.

[10] A. Belhocine, A.R. Abu Bakar, M. Bouchetara, Thermal and structural analysis of disc brake assembly during single stop braking event, Aust. J. Mech. Eng. 14 (1) (2016) 26–38.

[11] R.A. García-León, N. Afanador-García, J.A. Gómez-Camperos, Numerical Study of Heat Transfer and Speed Air Flow on Performance of an Auto-Ventilated Disc Brake, Fluids 6 (4) (2021) 160.

[12] A. Vdovin, M. Gustafsson, S. Sebben, A coupled approach for vehicle brake cooling performance simulations, Int. J. Therm. Sci. 132 (2018) 257–266, https:// doi.org/10.1016/j.ijthermalsci.2018.05.016.

[13] Habtamu Dubale, Velmurugan Paramasivam, Eneyw Gardie, Ewnetu Tefera Chekol, Senthil Kumaran Selvaraj. Numerical investigation of thermo-mechanical properties for disc brake using light commercial vehicle. Materials Today: Proceedings, 2021. ISSN 2214-7853.

[14] H.B. Yan, S.S. Feng, X.H. Yang, T.J. Lu, Role of cross-drilled holes in enhanced cooling of ventilated brake discs, Appl. Therm. Eng. 91 (2015) 318–333, https://doi.org/10.1016/j.applthermaleng.2015.08.042.

[15] L. Qiu, H.S. Qi, A. Wood, Two-dimensional finite element analysis investigation of the heat partition ratio of a friction brake, Proc. Inst. Mech. Eng. Part J J. Eng. Tribol. 232 (2018) 1489–1501, https://doi.org/10.1177/1350650118757245.

[16] H. Hong, G. Kim, H. Lee, J. Kim, D. Lee, M. Kim, M. Suh, J. Lee, Optimal location of brake pad for reduction of temperature deviation on brake disc during high-energy braking, J. Mech. Sci. Technol. 35 (2021) 1109–1120, https://doi.org/10.1007/s12206-021-0224-x.

[17] R. Jafari, K.T. Erkılıç, O. Tekin, R. Akyüz, M. Gürer, Experimental and numerical study of turbulent flow and thermal behavior of automotive brake disc under repetitive braking, Proc. Inst. Mech. Eng. - Part D J. Automob. Eng. (2021), https://doi.org/10.1177/09544070211040349.

[18] S. Topouris, Stamenković, D., Olphe-Galliard, M., Popović, V., Tirovic, M., Heat dissipation from stationary passenger car brake discs, Stroj. Vestn./J. Mech. Eng. 66 (2019) 15–28.

[19] S.B. Park, K.S. Lee, D.H. Lee, An investigation of local heat transfer characteristics in a ventilated disc brake with helically flfluted surfaces, J. Mech. Sci. Technol. 21 (2007) 2178–2187.

[20] M. Duzgun, Investigation of thermo-structural behaviors of different ventilation applications on brake discs, J. Mech. Sci. Technol. 26 (2012) 235–240.

[21] A. Belhocine, A. Afzal, FEA Analysis of coupled thermo-mechanical response of grey cast iron material used in brake discs, Rev. Cient. 3 (2019) 280–296.

[22] S. Lakkam, K. Suwantaroj, P. Puangcharoenchai, S. Mongkonlerdmanee, S. Koetniyom, Study of heat transfer on front-and back-vented brake discs, Songklanakarin Journal of Science and Technology 35 (2013) 671–681.

[23] SAE Tech. Pap. 4970 (2009), https://doi.org/10.4271/2009-01-3049.

[24] A. Coulibaly, N. Zioui, S. Bentouba, S. Kelouwani, M. Bourouis, Use of thermoelectric generators to harvest energy from motor vehicle brake discs, Case Stud. Therm. Eng. 28 (2021), 101379, https://doi.org/10.1016/j.csite.2021.101379.

[25] C. Qian, Aerodynamic shape optimization using CFD parametric model with brake cooling application, SAE Tech. Pap. (2002), https://doi.org/10.4271/2002-01-0599.

[26] A. Modanloo, M.R. Talaee, Analytical thermal analysis of advanced disk brake in high speed vehicles, Mech. Adv. Mater. Struct. 27 (2020) 209–217, https://doi.org/10.1080/15376494.2018.1472340.

[27] J.A. Standard, Passenger Car—Braking Device—Dynamometer Test Procedures, JASO C406 (2000) 1–9.

[28] J. Antony, D. Perry, C. Wang, M. Kumar, An Application of Taguchi Method of Experimental Design for New Product Design and Development Process, Assem. Autom. 26 (1) (2006) 18–24.

[29] Tirovic, M. (2013). Thermal effects in brakes, Braking of Road Vehicles 2013. Bradford University.

[30] Day, A. J., & Newcomb, T. P. (1984). The dissipation of frictional energy from the interface of an annular disc brake. proceedings of the institution of mechanical engineers, part D: transport engineering, 198(3), 201-209.

[31] M. Yilmaz, H. Köten, E. Çetinkaya, Z. Coşar, A comparative CFD analysis of NACA0012 and NACA4412 airfoils, Journal of Energy Systems 2 (4) (2018) 145–159.

[32] Köten, h., CFD modeling and multi-objective optimization of the axial fan parameters, Journal of Energy Systems 2 (4) (2018) 137–144.
[33] M. Sahbaz, A. Kentli, H. Köten, Thermal analysis and optimization of high power led armature, Therm. Sci. 23 (2A) (2019) 637.
[34] Y.H. Lee, M. Amran, Y.Y. Lee, A.B.H. Kueh, S.F. Kiew, R. Fediuk, N. Vatin, Y. Vasilev, Thermal Behavior and Energy Efficiency of Modified Concretes in the Tropical Climate: A Systemic Review, Sustainability 13, no. 21 (2021) 11957, https://doi.org/10.3390/su132111957.
[35] Y.H. Lee, N. Chua, M. Amran, Y.Y. Lee, A.B.H. Kueh, R. Fediuk, N. Vatin, Y. Vasilev, Thermal Performance of Structural Lightweight Concrete Composites for Potential Energy Saving, Crystals 11, no. 5 (2021) 461, https://doi.org/10.3390/cryst11050461.
[36] M.B. Hossain, M. Roknuzzaman, M.A. Biswas, M. Islam, Evaluation of engineering properties of thermal power plant waste for subgrade treatment, Journal of Civil Engineering, Science and Technology 12 (2) (2021) 112–123.
[37] Y.X. Tang, Y.H. Lee, M. Amran, R. Fediuk, N. Vatin, A.B.H. Kueh, Y.Y. Lee, Artificial Neural Network-Forecasted Compression Strength of Alkaline-Activated Slag Concretes, Sustainability 14, no. 9 (2022) 5214, https://doi.org/10.3390/su14095214.
[38] J. Zhou, J. Sun, W. Zhang, Z. Lin, Multi-view underwater image enhancement method via embedded fusion mechanism, Eng. Appl. Artif. Intel. 121 (2023), 105946.
[39] J. Zhou, L. Pang, W. Zhang, Underwater image enhancement method by multi-interval histogram equalization, IEEE J. Ocean. Eng. 48 (2) (2023) 474–488.